

Supporting information for “A study of film structure and adsorption kinetics of polyelectrolyte multilayer films: effect of pH and polymer concentration” by Garg *et al.*

Ellipsometry Procedure

Film thickness measurements were made using a variable angle spectroscopic ellipsometer (VASE) (J.A. Woolam ellipsometer VB-200 with WVASE32 software version 3.361). Ellipsometry is based on the changes in the polarization of light when it reflects from a surface. Linearly polarized light reflects off the sample and becomes elliptically polarized. This change in the state of polarization can be defined by two quantities, namely Δ (delta) and ψ (psi)¹. The phase difference between the linearly polarized light and the elliptically polarized light is given by Δ whereas ψ gives the change in amplitude between the two. The ellipsometric analysis was done in the vicinity of the Brewster angle because ellipsometry measurements are most sensitive to film characteristics at the Brewster angle². An initial scan was done for wavelengths from 300 to 800 nm at 50 nm intervals and this wavelength range was then repeated over angles from 50 deg to 70 deg at 4° intervals to find the Brewster angle. From a graph of Δ vs. λ , Brewster angle was determined as the point at which Δ quickly passed from 180° through 90° to 0°². The Brewster angle for PAH/PCBS slide series was found to be 62°. Following the determination of the Brewster angle, the sample was scanned at wavelengths from 300 to 800 nm at 10 nm intervals in the vicinity ($\pm 2^\circ$) of the Brewster angle in 1° increments. The experimental data collected this way were then fitted with a model that is described below in detail. Using this approach, for each film, the thickness was calculated at three different positions using the Lorentz oscillator model described below. From the resulting thicknesses, an average thickness per bilayer was calculated along with the standard deviation.

Modeling

The model consists of two layers - one for the glass substrate and the other for the thin film. The model for the glass substrate consists of the refractive index and the

extinction coefficient (n and k respectively) values as a function of wavelength and is plotted in Figure 1 below.

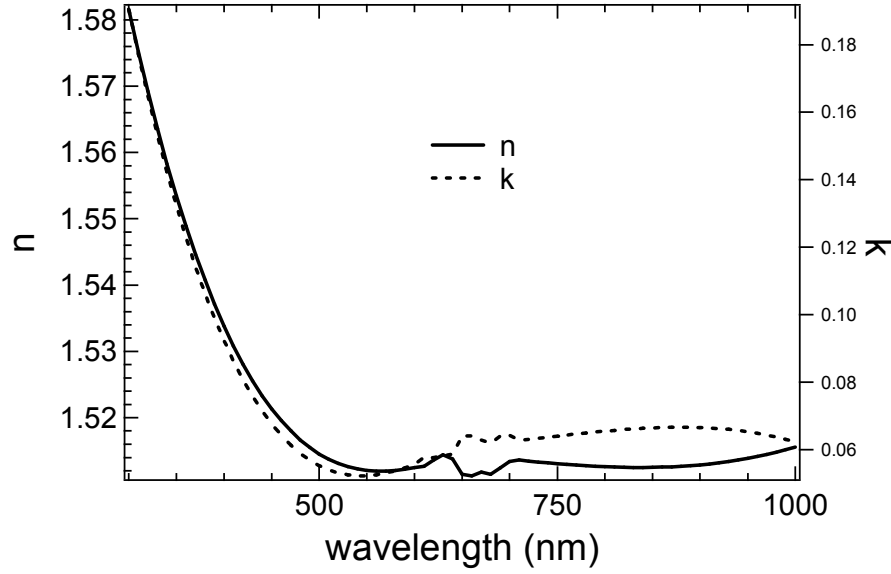


Figure 1. n and k values versus wavelength for a typical glass substrate used in the film deposition experiments. These values were used to model the experimental data for the ISAM films.

The Lorentz oscillator model represents the thin film and is given by the following equation²:

$$\varepsilon(E) = \varepsilon_1(\infty) + \sum_k \frac{A_k}{E_k^2 - E^2 - iB_k E} \quad (1)$$

where, $\varepsilon_1(\infty)$ represents the value of the real part of the dielectric function at very large photon energy, A_k is the amplitude of the k^{th} oscillator (eV^2), E is the photon energy (eV), E_k is the center energy of the k^{th} oscillator (eV), and B_k is the k^{th} peak's width (eV). E_k is given by equation (2). From ε , values of n and k can be calculated as shown in equations (3) and (4).

$$E_k = h\nu_k = \frac{1.24(\text{eV} \cdot \mu\text{m})}{\lambda_k(\mu\text{m})} \quad (2)$$

$$n = \sqrt{\frac{\varepsilon_1 + \sqrt{\varepsilon_1^2 + \varepsilon_2^2}}{2}} \quad (3)$$

$$k = \sqrt{\frac{-\varepsilon_1 + \sqrt{\varepsilon_1^2 + \varepsilon_2^2}}{2}} \quad (4)$$

where ν_k and λ_k are the frequency and the wavelength of the k^{th} absorbance peak, respectively. A typical value of λ_k (as measured by UV-Vis spectroscopy) for PAH/PCBS slide series is 360 nm.

Because only one absorbance peak was observed while scanning the slide for absorbance over a range of wavelength, only one Lorentz oscillator model was used and its oscillating center was fixed at $\lambda_k (= \lambda_1)$. Using the above value for λ_1 , the parameter E_1 can be calculated from equation (2). The value for the parameter E_1 for the PAH/PCBS films was calculated to be 3.444 eV.

An initial guess was provided for the other parameters ε_∞ , A_1 and B_1 to estimate the film thickness. Depending on the initial guess provided, the results might vary. However, there are various ways to determine if the obtained results were optimal. One of the constraints in fitting the parameters is that k should reach a maximum at λ_1 . The goodness of fit was assessed with the values of the mean sum of the errors (MSE). In general, a better fit is obtained with lower values of the MSE. The optical parameters obtained after modeling are shown in the Figure 2 for the films made using PCBS and PAH.

When making the films, PAH and PCBS solutions were used with a concentration of 10 mM based on their repeat units and at pH 7. The glass slides were dipped in PAH and PCBS solutions for 2 minutes. The rinsing time after each dipping cycle was 135 sec.

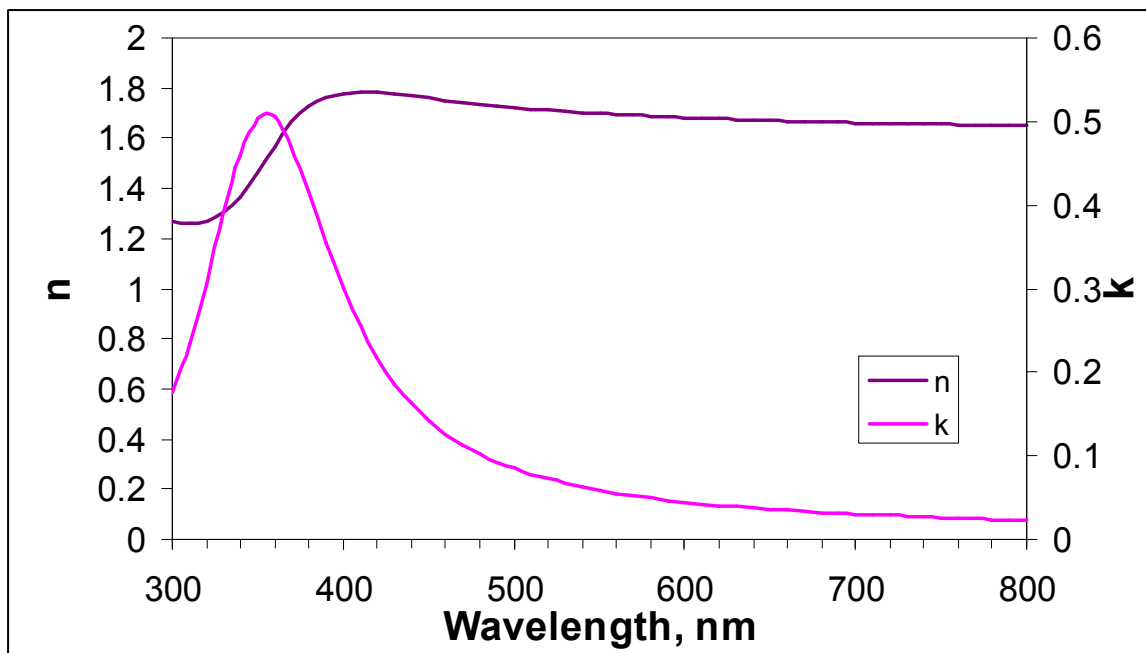


Figure 2. Optical parameters for a film consisting of 500 bilayers of PAH/PCBS obtained using VASE. The deposition conditions were: $C_{\text{PAH}} = 10$ mM repeat unit (RU), $C_{\text{PCBS}} = 10$ mM RU, $\text{pH}_{\text{PAH}} = 7.0$, $\text{pH}_{\text{PCBS}} = 7.0$. The dipping times were 2 minutes in both PAH and PCBS solutions. The rinsing time was 135 seconds equally distributed in three baths (45 sec x 3). The maximum value of the dispersion coefficient occurs at the wavelength ~ 360 nm. A similar peak is observed at this wavelength by UV-Vis spectroscopy.

Design of flow loop for QCM experiments

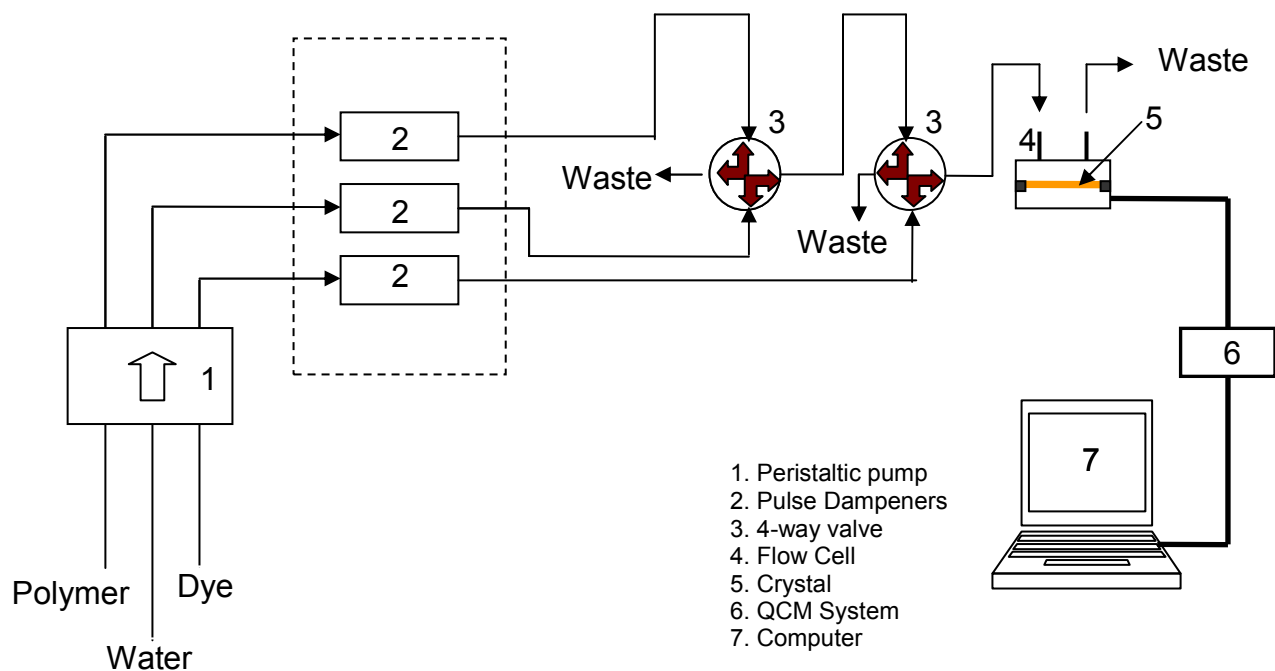


Figure 3. The experimental set-up for experiments done using Maxtek's QCM. Peristaltic pump is used to control the flow rates at which the solutions are passed. Pulse dampeners are used to virtually eliminate pulsations caused by peristaltic pump. The solutions are then passed through a system of two 4-way valves and the tubes are connected such that there is always a constant flow of solutions. One of the outlets through the system of valves goes to the QCM flow cell. The QCM crystal is placed inside the QCM flow cell and only one surface comes in contact with the solution. The change in frequency as a function of time is monitored through a computer connected to the QCM electronics via a serial port.

The flow loop system used with the QCM is shown in Figure 3. The experimental set up consisted of: a peristaltic pump, three pulse dampeners, two 4-way valves, the QCM flow cell and electronics. The peristaltic pump was used to provide a continuous flow over a range of 0.6 ml/min to 10 ml/min and was connected to multiple pump heads through which three different fluids were passed. Each of the tube lines then went through a pulse dampener (Cole Parmer) which mostly eliminated the pulsation caused by the peristaltic pump. Uttenthaler et al.³ used pulse dampeners to decrease the pulsation

caused by a peristaltic pump. The pulse dampeners were very useful for our experimental set up because of the sensitivity of the QCM to even very small pressure pulses. The tube then went to a system of two 4-way valves arranged so that the pumping through all three lines was continuous throughout the duration of the experiment. This was done to keep the pressure the same in all the lines at all times. One of the output lines through the valve system went into the QCM flow cell and the other two lines went to waste or were recycled as needed. The QCM flow cell has a volume of 0.1 ml. It took almost 2 hours for the Maxtek QCM to warm up and give a stable baseline. For the experiments done with the crystal in contact with liquid, the crystal was first allowed to stabilize in air and a reading in air was recorded to see the noise and drift levels in air and then the liquid was introduced.

Higher harmonics from the QCM-D data.

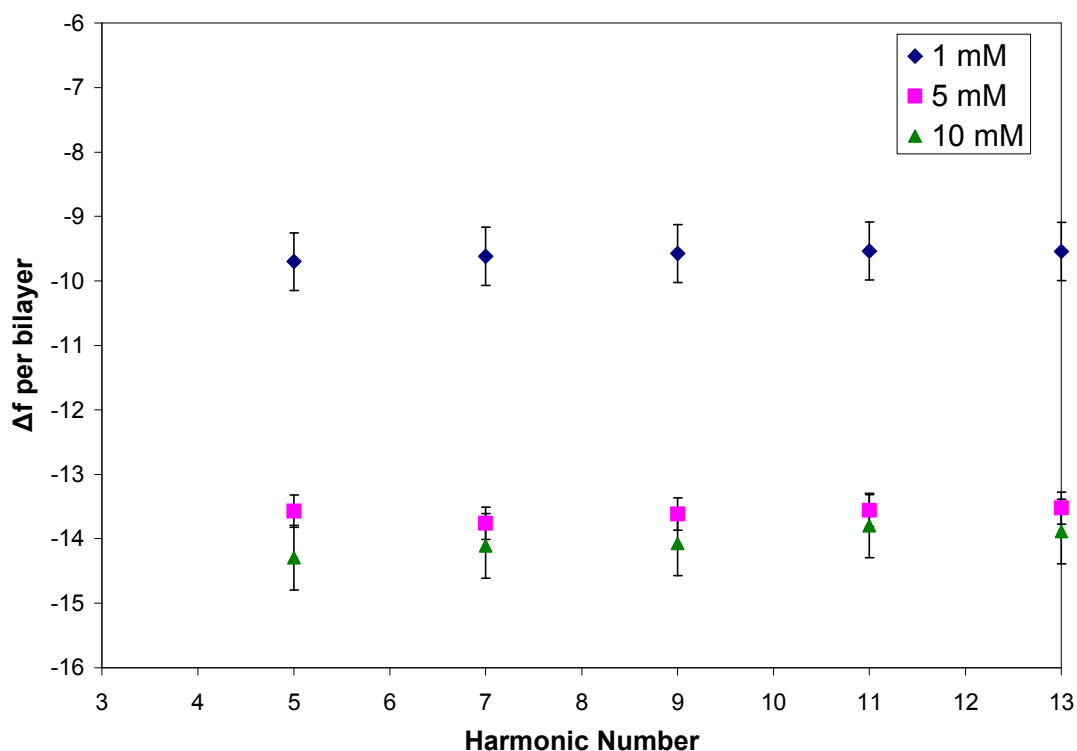


Figure 4. Change in frequency per bilayer for QCM-D at different harmonics for deposition conditions at three different polymer concentrations and for PAH and PCBS pH = 7.

Voigt Model

The Voigt model ⁴⁻⁶ which is based on a spring and dashpot connected in parallel can be used to estimate the thickness and mechanical properties such as the viscosity and shear modulus of the adsorbed films. In the Voigt model, the complex shear modulus of the film is given by: ⁷

$$\mu^* = \mu_h + i2\pi f \eta_h \quad (5)$$

where μ_h is the elastic shear modulus and η_h is the shear viscosity of the film. The characteristic relaxation time $\tau = \eta_h / \mu_h$ (see eq 4 in paper). The film is assumed to lie in contact between the QCM electrode and a semi-infinite Newtonian liquid under no-slip conditions and is represented with a uniform thickness t_h and a density ρ_h , referred to as the effective hydrodynamic thickness and density, respectively. In this case, the changes in the resonant frequency Δf and the dissipation factor ΔD are:

$$\Delta f = \frac{\text{Im}(\beta)}{2\pi t_q \rho_q} \text{ and } \Delta D = -\frac{\text{Re}(\beta)}{\pi f t_q \rho_q} \quad (6)$$

where t_q and ρ_q are the thickness and specific density of quartz plate and,

$$\beta = \xi_1 \frac{2\pi f \eta_h - i\mu_h}{2\pi f} \frac{1 - \alpha \exp(2\xi_1 t_h)}{1 + \alpha \exp(2\xi_1 t_h)} \quad (7)$$

$$\alpha = \frac{\frac{\xi_1}{\xi_2} \frac{2\pi f \eta_h - i\mu_h}{2\pi f} + 1}{\frac{\xi_1}{\xi_2} \frac{2\pi f \eta_h - i\mu_h}{2\pi f} - 1} \quad (8)$$

$$\xi_1 = \sqrt{-\frac{(2\pi f)^2 \rho_h}{\mu_h + i2\pi f \eta_h}}, \quad \xi_2 = \sqrt{i \frac{2\pi f \rho_1}{\eta_1}} \quad (9)$$

where ρ_h and ρ_l are the density of the hydrated film and bulk liquid, respectively, η_h and η_l are the viscosity of the hydrated film and the bulk liquid, respectively, and μ_h is the elastic modulus of the hydrated film. For an aqueous environment, ρ_l and η_l are approximately 1.0 kg m^{-3} and 1.0 Ns m^{-2} , respectively. In air, the viscosity remains essentially the same, but the density is a factor of about 1×10^3 lower.

For thin films, the above equations for Δf and ΔD can be expressed in simpler forms by a Taylors series expansion: ⁴

$$\Delta f \approx -\frac{1}{2\pi\rho_q t_q} t_h \rho_f \omega \left(1 + \frac{2t_h^2 \chi}{3\delta^2(1+\chi^2)} \right) \quad (10)$$

$$\Delta D \approx \frac{2t_h^3 \rho_h \omega}{3\pi f \rho_q t_q} \frac{1}{\delta^2(1+\chi^2)} \quad (11)$$

where t_h and ρ_h are the thickness and specific density of the hydrated film and

$$\chi = \frac{\mu_h}{\eta_h \omega} \quad \text{and} \quad \delta = \sqrt{\frac{2\eta_h}{\rho_h \omega}}.$$

Equations (10) and (11) are the main equations that describe the Voigt model for thin films.

We used the Voigt model to estimate the thicknesses of the adsorbed PAH and PCBS bilayers. To do these calculations, three parameters need to be specified: the film density (ultimately calculated to be 1100 kg/m^3) and the density and viscosity of the solvent, in the present case taken to be that of water at 25°C , 1000 kg/m^3 and 0.001 Pa s , respectively.

A comparison of the hydrated film thickness calculated from the Voigt model and the Sauerbrey equation

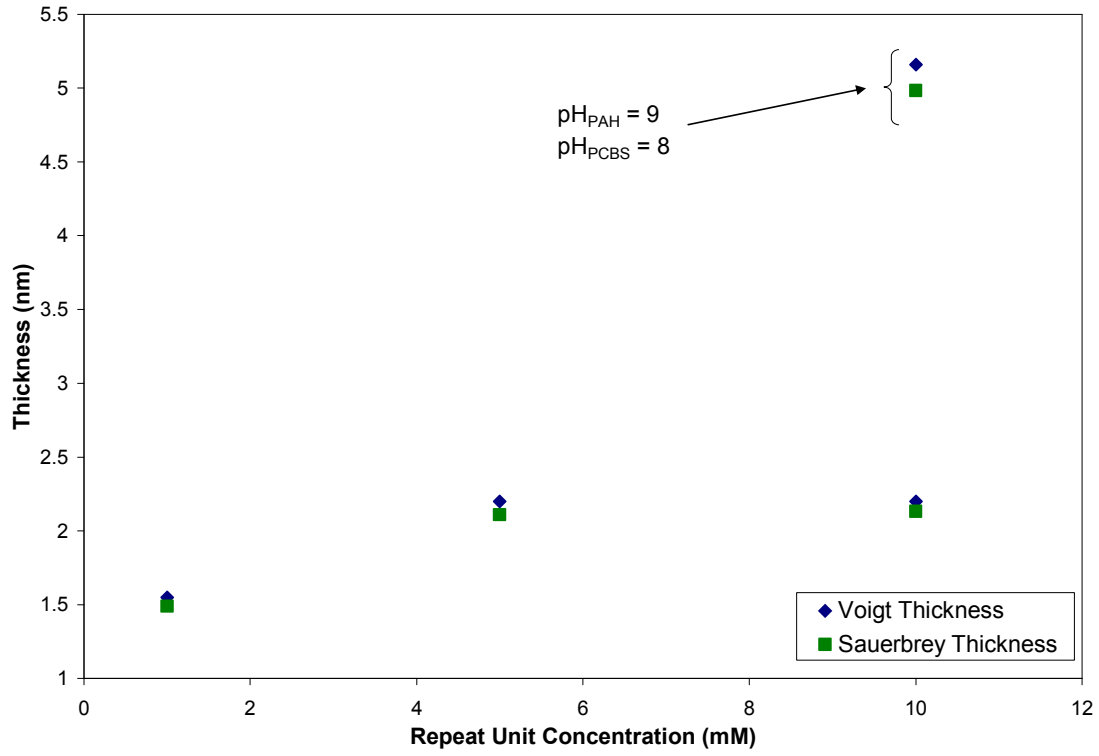


Figure 5. A comparison of thickness t_h obtained by the Voigt model and Sauerbrey equation [equation (2) in paper] for different deposition conditions. For deposition condition: (PAH-10/PCBS-10)_{9/8}, the data points are marked by an arrow; whereas, for deposition conditions (PAH-1/PCBS-1)_{7/7}, (PAH-5/PCBS-5)_{7/7}, (PAH-10/PCBS-10)_{7/7} the data points are not marked by an arrow.

Table S1. A comparison of the water content of films calculated using the Voigt model and using the Sauerbrey equation

Conc.	$-(\Delta f)$ per bilayer	Mass per unit area, m_w (mg/m ²) wet*	Thickness of dry film from ellipsometry, t_d (nm)	Mass per unit area, m_d (mg/m ²) dry**	% water*** (Compare with Table 4 in the paper)	% deviation from water content calculated using Voigt model see paper
1	9.27	1.64	0.77	0.92	43.68	4.6
5	13.27	2.35	1.20	1.42	38.69	4.5
10	13.51	2.39	1.16	1.39	41.78	1.7

* Calculated using the Sauerbrey equation [equation (2) in paper]

** Calculated from the dry film thickness by assuming a density of 1200 kg/m³ for dry films^{8, 9}

*** Calculated using equation % water = $[(m_w - m_d)/m_w] \times 100$

References:

1. Azzam, R.M.A.; Bashara, N.M., *Ellipsometry and Polarized Light*, North-Holland Personal Library; 1987.
2. Tompkins, H.G.; McGahan, W.A., *Spectroscopic Ellipsometry and Reflectometry*, Wiley Interscience; Chapter 2, (1999).
3. Uttenthaler, E.; Schraml, M.; Mandel, J.; Drost, S., Ultrasensitive quartz crystal microbalance sensors for detection of M13-Phages in liquids. *Biosensors & Bioelectronics* **2001**, 16, 735-743.
4. Voinova, M. V.; Rodahl, M.; Jonson, M.; Kasemo, B., Viscoelastic Acoustic Response of Layered Polymer Films at Fluid-Solid Interfaces: Continuum Mechanics Approach. *Phys. Scr.* **1999**, 59, 391-396.
5. Rodahl, M.; Kasemo, B., On the measurement of thin liquid overlayers with the quartz-crystal microbalance. *Sensors and Actuators A* **1996**, 54, 448-456.
6. Ferry, J. D., *Viscoelastic properties of polymers*. Third ed.; John Wiley and Sons, Inc.: 1980.
7. Hook, F.; Larsson, C.; Fant, C., Biofunctional Surfaces Studied by Quartz Crystal Microbalance with Dissipation Monitoring. *Encyclopedia of Surface and Colloid Science* **2002**, 774-791.

8. Caruso, F.; Niikura, K.; Furlong, D. N.; Okahata, Y., Ultrathin Multilayer Polyelectrolyte Films on Gold: Construction and Thickness Determination. *Langmuir* **1997**, 13, 3422-3426.
9. Lvov, Y.; Ariga, K.; Onda, M.; Ichinose, I.; Kunitake, T., A Careful Examination of the Adsorption Step in the Alternate Layer-by-Layer Assembly of Linear Polyanion and Polycation. *Colloids and Surfaces A: Physiochemical and engineering aspects* **1999**, 146, 337-346.